

Article

Use of Webcams in Support of Operational Snow Monitoring

Cemal Melih Tanis ^{*}, Elisa Lindgren, Anna Frey, Lasse Latva , Ali Nadir Arslan  and Kari Luojus

Finnish Meteorological Institute (FMI), P.O. Box 503, FI-00101 Helsinki, Finland

^{*} Correspondence: cemal.melih.tanis@fmi.fi

Abstract: Ultrasonic sensors are one of the most common automatic monitoring methods in operational snow depth monitoring with reliable results. On the other hand, there is significant uncertainty when measuring small snow depths (<2 cm), thus it cannot provide binary snow presence (on/off) information. The use of webcams in monitoring snow cover has proven to be successful in recent studies and applications. In this study, we applied an adaptive thresholding technique on images from webcams to obtain reliable snow on/off information to complement the ultrasonic snow depth measurements. Camera and ultrasonic sensor data from two weather stations in Finland were studied. The webcam data was processed using FMIPROT (Finnish Meteorological Institute Image Processing Tool) software, operating in a cloud computing environment, which can generate near real-time data. Our results indicate that webcam-derived data can be successfully used for quality control or as auxiliary data to support operational ultrasonic sensor measurements and provide a cost-effective improvement to operational monitoring capabilities. Webcam monitoring is especially useful during the melting season when the snow depth is below 15 mm, with accuracy values between 72% and 94%.

Keywords: snow cover; snow depth; webcam monitoring; ultrasonic measurement; cloud processing; computer vision; operational monitoring



Citation: Tanis, C.M.; Lindgren, E.; Frey, A.; Latva, L.; Arslan, A.N.; Luojus, K. Use of Webcams in Support of Operational Snow Monitoring. *Geosciences* **2023**, *13*, 92. <https://doi.org/10.3390/geosciences13030092>

Academic Editors: Mohammad Valipour and Jesus Martinez-Frias

Received: 14 February 2023

Revised: 11 March 2023

Accepted: 18 March 2023

Published: 22 March 2023



Copyright: © 2023 by the authors. Licensee MDPI, Basel, Switzerland. This article is an open access article distributed under the terms and conditions of the Creative Commons Attribution (CC BY) license (<https://creativecommons.org/licenses/by/4.0/>).

1. Introduction

Ultrasonic sensor (US) based snow cover measurement instruments emit acoustic waves toward the ground and interpret the reflected wave to measure snow depth. They have been the primary method of measuring snow depth in the meteorological community in recent decades [1]. Present operative snow depth US technique (SR50AH, Campbell Scientific) at the Finnish Meteorological Institute (FMI) lacks the possibility to recognize snow presence reliably in the cases where snow depth (SD) is very low (<2 cm) or if there are leaves, sticks or other roughness on the snow bed area. Internal user questionnaires were conducted in FMI to investigate the interest in snow cover information in operational monitoring databases. Based on the questionnaires, snow presence information over an area has been recognized to be usable information for various application areas of meteorological services. Visually estimated in-situ state of ground information provided once per day is already operationally available but the need for additional methods to obtain the state of snow cover on the ground is clear.

Digital imagery from environmental camera networks can be used in image processing techniques to estimate snow cover and snow depth. Using contour detection over the images of snow sticks to detect snow depth was studied by [2]. The results show that the method is reliable in general, but not reliable for snow depth below 2 cm. An adaptive thresholding method applied on images from digital cameras to obtain fractional snow cover information was studied before by [3] in the Alps and Apennines and later in northern boreal conditions by [4]. Although there are challenges to estimate the snow cover correctly in certain weather conditions, it is possible to obtain snow cover information in the long term using the adaptive thresholding method. Snow presence derived from fractional snow cover information extracted from camera images as an add-on to the snow depth

measurements from US can be a cost-effective solution to the measurement gap in low snow depth cases.

In this paper, it is investigated whether the snow cover fraction information extracted from digital imagery can be useful and provide added value to the US snow depth measurements. Snow depth measurements, digital imagery, and visual inspections (through images) from two weather stations are used. Reliability of the image processing results are assessed using visual inspections. The assessment is conducted in different cases of snow depth and snow cover presence to determine in which conditions the data can be used. The digital imagery is processed in near real time using the FMI Image Processing Toolbox (FMIPROT) & Camera Network Portal and the extracted values are fed to the operational observation database of the FMI [5].

2. Materials and Methods

2.1. Stations

The stations for the study represented the typical snow circumstances in southern and northern Finland. The site locations were chosen based on the infrastructure available. Jokioinen Ilmala is located inland in the southern part of the country. There, the typical number of days with snow cover (1991–2020 normal period) is 115–130 [6]. At the station in the northern part of Finland, Sodankylä Tähtelä (test field, Solid Precipitation Intercomparison Experiment (SPICE) were conducted here 2012–2015 [7]), the corresponding number of snow-covered days is 175–190 [6]. In southern Finland, the starting and ending of the snow cover season are usually more unstable than in northern Finland, leading to a higher number of changes in the snow on/off cases in the southern part of the country than in north. The locations of the stations are shown on a map of Finland in Figure 1. The stations and the close surroundings can be seen from the camera views in Figure 2, for (a) Jokioinen and (b) Sodankylä.



Figure 1. The locations of the stations in Finland.



Figure 2. Web camera images of weather station setups in (a) Jokioinen and (b) Sodankylä. The areas with yellow marking are the chosen ROIs.

2.1.1. Jokioinen

The Jokioinen Ilmala station is located around 100 km inland from the southern coast of Finland (60.81397222° N, 23.49825° E). The surrounding areas of the stations are mainly cultivated lands with some low forested hills.

The site has an operative automatic weather station (AWS) where the US snow depth observations are operated as part of the operative AWS. The best practices for fulfilling the requirements, and recommendations of the World Meteorological Institute in [8] are implemented for the operational observations, noticing the requirements set by the local conditions. An Axis Q6035-E network dome camera was installed specifically for this study.

2.1.2. Sodankylä

Sodankylä station is located in Finnish Lapland (67.367764° N, 26.632931° E) at the Finnish Meteorological Institute's Arctic Research Centre in a boreal environment. The areas surrounding the station are covered by peatlands and boreal coniferous forest. The river Kitinen runs to the west of the station. Snow covers the ground from October to April [9].

The snow depth observations and camera were available from the testing field where the infrastructure was previously built for the SPICE project [7]. The infrastructure of the snow depth observations corresponds to the operative one that is described in the chapter "Ultrasonic Sensors and snowbed area". The images were taken using an Axis Q6035-E network dome camera.

2.2. Camera Imagery

The camera images are stored in JPEG format with 1920×1080 pixels (Full HD) resolution, which results in image files between 100–500 KB. The cameras are connected to the FMI network, and they upload their images to an internal server enabling FMIPROT software to retrieve them automatically. The cameras from both stations capture and upload one image each hour.

2.3. Ultrasonic Sensors and Snowbed Area

In this study, the instrument observing the snow depth was an ultrasonic sensor (US) SR50AH of Campbell Scientific Ltd., 80 Hathern Road, Shepshed, Loughborough, UK. The ultrasonic snow depth measurement is a distance calculation based on measuring the time that it takes for the ultrasonic pulse to propagate and reflect from the surface back to the sensor. The SR50A sensor uses a 50 kHz electrostatic transducer and the sensor internally compensates for the speed of sound variation in the air (dependent on temperature) [10]. The snowbed areas under the ultrasonic sensors were green colored artificial turfs, with sizes of about 2 m by 2 m (see Figure 2).

2.4. Visual Inspections

The hourly snow presence was visually inspected from the images for the period starting in November 2020 and ending after the melting season of Spring 2021. The snow presence created by the visual inspection was categorized based on the values (0–4) shown in Table 1. The meaning of the categories is explained in the “Label” column of Table 1. The visual inspection for the pictures was made by two observers. The observers were experts at the airport who were on duty to observe the meteorological conditions at the airport. For the inspection of this study, they were equally trained to estimate the state of the ground for the purpose of the FSC comparison. Each picture was inspected by only one person and each picture obtained a value from 0 to 4, depending on the estimation of the observer. The FSC hourly data were compared with the visually inspected snow categories after they were classified to the corresponding classes shown in the last column (Percent) of Table 1. It must be noted that the visual inspection also represented the surrounding area in the images, not only the snowbed area. In addition, the fact that each picture was inspected by only one person increases the uncertainty of the estimation.

Table 1. Correspondence between visual inspection of snow scale and FSC limits.

Snow Presence		FSC
Category	Label	Percent
0	NULL (e.g., unclear picture)	-
1	no snow	0–10
2	ground partly covered by snow	10 < FSC < 90
3	full snow cover	90–100
4	frost or ice	-

2.5. Estimating FSC from Digital Imagery

The FSC is estimated from the digital imagery by the application of the adaptive thresholding algorithm studied in [4]. The algorithm is applied on a selected ROI which covers a portion of the turf in the camera’s view, where the US measurements are taken. The selected ROIs are presented in Figure 2. The algorithm uses the pixel values in the blue channel inside the ROI to determine a threshold, depending on the histogram of the values. The first local minimum, after the half of the maximum pixel value, is selected as the threshold. If a minimum cannot be found, then the FSC cannot be estimated. The pixels with the blue channel value above the threshold are determined as snow covered. Then, the FSC is calculated by applying the georectification on the image and considers the different area sizes that the pixels represent but for this study, georectification is not applied as the positions, the distance and sizes of the ROIs do not cause a considerable difference for the FSC to be evaluated for snow presence.

For the detection algorithm, having a meaningful histogram of the values requires a level of brightness in the ROI. Thus, before applying the algorithm, images are filtered according to the brightness of the images. The brightness is calculated as the ratio of the average value of pixels to the maximum possible value of the pixels [5]. The thresholds are decided empirically, according to the time series of the brightness values. The brightness and the FSC time series, without the filtering, is plotted together for this decision. The FSC values are unstable (changing between 0% or 100%) when the brightness is very low. This is an effect which can be visible at values at dusk and dawn times from such a plot. For both the cameras, the brightness threshold is decided as 0.45 (45%) using that method. Depending on the camera and the camera settings, such as automatic contrast or automatic white balance; the white balance may happen to be significantly different than normal in the pictures (i.e., image looking very blue, red, or green). This happens sometimes when the overall contrast is high (e.g., when the snow cover is high and sun illumination is low). In that case, the histogram of the blue channel is also not meaningful for the algorithm. Thus, such images are filtered according to the blue fraction (BF) of the images, which is

calculated as the ratio of the average blue channel value to the sum of the average values of all the channels [5]. The thresholds are decided empirically, according to the time series of the BF values. For the Sodankylä camera, such a case does not happen, thus no filtering is applied. For the Jokioinen camera, the BF thresholds are decided as 0.325 and 0.34, so that the BF is always inclusively between those values. The example images from the Jokioinen camera for filtering by brightness and the blue fraction are shown in Figure 3.

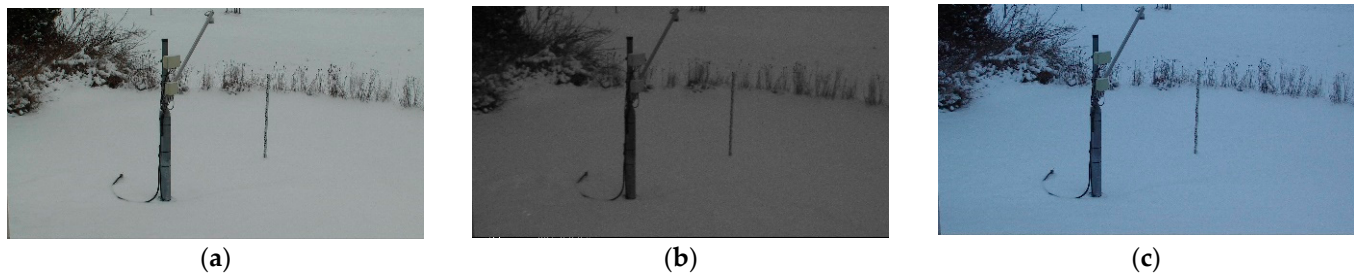


Figure 3. Example images from Jokioinen camera for filtering by brightness and blue fraction: (a) nominal; (b) low brightness; (c) high blue fraction.

The FSC data are produced by the FMIPROT (V. 0.24) software. The toolbox performs the necessary tasks to acquire images from the image repositories of the camera networks, processing them and generating the output data as well as the HTML reports along with interactive plots for the visualization of the output data [5].

2.6. Cloud-Based NRT Processing

The FMIPROT software is the core of the backend of the FMIPROT & Camera Network Portal. The software is run through different scripts, which are triggered by a job scheduler. The scripts manage the curation of the latest images from the camera network images, where available, to present them on the webpage and process the images according to the setups, which generate snow cover and vegetation data from the selected cameras. All the acquisitions and processing are performed in NRT, according to the timeliness selected for each setup. The output data, in the time series, are visualized in interactive plots and maps, and the raw data are also available through a form and a basic HTTP API.

The portal has different setups from the different projects. For this study, the setups with the name “LumiPilotti” for the latest one month of data (running each 10 min) and “LumiPilottiAll” for the latest one year of data (running each month) are created. These setups are created using FMIPROT in a workstation and then the setup files are uploaded to the server. The selections in the setup files are accessible through the portal (via “Setup report” links), which makes it possible to reproduce or replicate the output data, when access to the imagery is provided. Currently, the images from the cameras, which are used in the study are available only from the FMI network.

2.7. Comparison of FSC from Camera Imagery vs. Visual Inspection

The FSC data derived from the camera imagery is compared with the snow presence data observed by the visual inspection. The snow presence in the visual inspection was categorized and the FSC values were classified to the corresponding classes based on the values shown in Table 1. The FSC hourly data was compared with the visually inspected snow categories. It must be noted that the visual inspection also represented the surrounding area in the images, not only the snowbed area.

The data are temporally divided into three sets for two hydrological years: melting season, winter snow season, and the beginning of the snow season. The number of cases which correspond to the category for each source of data are recorded in Tables 2 and 3. This comparison is conducted to see the overall agreement between the data sources, and no metrics are calculated.

Table 2. The correspondence between visual inspection of snow presence and FSC data in Sodankylä (ROI the whole snowbed).

Visual Ins. Category	17.10.2020–4.12.2020 Beginning Season			4.12.2020–1.4.2021 Winter Season			1.4.2021–18.5.2021 Melting Season		
	FSC Cat. 1	FSC Cat. 2	FSC Cat. 3	FSC Cat. 1	FSC Cat. 2	FSC Cat. 3	FSC Cat. 1	FSC Cat. 2	FSC Cat. 3
0	0	0	0	0	0	0	0	0	0
1	0	0	0	0	0	0	1	1	0
2	0	0	7	0	0	0	21	107	81
3	3	3	62	35	145	647	1	58	266

Table 3. The correspondence between visual inspection of snow presence and FSC data in Jokioinen (ROI the whole snowbed).

Visual Ins. Category	25.12.2020–13.1.2021 Beginning Season			14.1.2021–1.3.2021 Winter Season			1.3.2021–15.4.2021 Melting Season		
	FSC Cat. 1	FSC Cat. 2	FSC Cat. 3	FSC Cat. 1	FSC Cat. 2	FSC Cat. 3	FSC Cat. 1	FSC Cat. 2	FSC Cat. 3
0	0	0	1	0	0	0	1	0	0
1	0	0	0	0	0	0	30	17	0
2	1	0	27	0	0	0	46	72	37
3	10	3	36	73	0	184	0	1	37

2.8. Comparison of FSC from Camera Imagery vs. SD from US

The comparison between the FSC from camera imagery and the SD from the SR50 sensor outputs was performed to study if the FSC could complement the SD information and even work as a cross-checking source for the operational snow depth observations in the automatic quality control (AQC) system. The analysis period started by and ended after the melting season of spring 2021 (March 2020–May 2021). The number of cases when the FSC and the SR50 data gave contradictory results was calculated to give an initial indication to see if the crosscheck between the FSC and the SD could be used as an AQC test. The FSC data produced by the image processing was compared with the SD observations produced by the US sensors at the beginning of the snow season, winter season, and melting season. The focus of the FSC vs. SD comparison analysis was to find contradictory cases to study to see if the case character and the amount could indicate whether the tested limits could be used for cross check definitions for the SD and FSC data. The FSC data are presented as percentages (%) of the snow in the ROI. In the operative use, the SD observations are defined as the following (accuracy 1 mm):

- $SD < 15 \text{ mm} \rightarrow SD = 0 \text{ mm}$
- $15 \text{ mm} \leq SD < 25 \text{ mm} \rightarrow SD = 20 \text{ mm}$
- $SD > 20 \text{ mm} \rightarrow 5 \text{ mm accuracy, e.g.,}$
 - 24 mm rounded to 20 mm.
 - 25 mm rounded to 30 mm.

For the operative production of the SD information, the main interest was to analyze if the SD, interpreted to be 0 mm (<15 mm), could be recognized as snow covered ground based on an FSC analysis. The SD cases of less than 15 mm (i.e., $SD = 0 \text{ mm}$ or very little snow) were compared with the FSC cases of higher than 0% and 10% (i.e., at least a little snow).

Also, the SD cases, that are higher than and equal to 15 mm (i.e., minimum of SD 20 mm), were compared with the FSC cases of 0% or less than or equal to 10% (i.e., no snow

or very little snow). This comparison could be useful in the cases where there are some leaves, sticks, or other roughness on the snowbed.

2.9. Assessment of Conditions Where Snow Cover Information Is Fit for Use

The correspondences of the FSC information and SD vs. FSC from the visual inspection of the snow presence were studied to estimate the accuracy of the FSC analysis to detect the snow cover correctly. The contradictory cases between the SD and FSC were divided into cases where the FSC agreed with and was contradictory with the snow presence estimation by the visual inspection.

2.10. Pilot the Transmission of the FMIPROT Information for the Future Operative Use

One goal of the study was to pilot the possibility to deliver FSC information from the FMIPROT server to the operational observation database of the FMI. The FSC messages were transmitted to the database by polling the image processing output files every five minutes. Each poll, the FMIPROT server lists all the relevant data and filters them for validity (e.g., nan values) and possible duplicates. The scripts also check if the point data were transmitted already. If the data are valid and new, the transmission to the database is performed by sending the ASCII messages over the TCP/IP. The message format was defined to correspond to the format needed for the FMI's ASCII message of the data collection procedure. The maximum allowed latency was set to 10 min as a rule to send only NRT messages.

Additionally, the selection of the cameras that are applied for publishing the FSC data are chosen using a configuration file in the operative database. Thus, the coverage can be modified continuously. If any new cameras are added to the system or existing data from the other cameras to be used for the FSC estimation, this file can be modified to include them in the transmission.

3. Results

3.1. Comparison of FSC from Camera Imagery vs. Visual Inspection

The results of the comparison between the visual inspection of snow presence (the classification is shown in Table 1) and the FSC results in Sodankylä and Jokioinen are shown in Tables 2 and 3, respectively.

In Sodankylä, the visual inspection and FSC estimation of snow presence mainly corresponded well with each other (Table 2). The biggest difference occurred within the winter season where the FSC seemed to predict a significant amount of no snow or partly snow cases even though the visual inspection showed full snow presence. Most probably in these cases, the images are not good enough for the image recognition as they include a number of shaded, unclear, or diffusely illuminated images [4].

The comparison of the snow presence predicted by the FSC and the visual inspection in Jokioinen (Table 3) showed more deviation than in Sodankylä. Within the beginning season, there were cases where the visual inspection revealed partly snow when the FSC gave full snow cover information. The same applied for the melting season but there was some deviation to the other combination as well. Within the melting season there were also cases where the FSC predicted no snow, but the visual inspection ended up to being partly snow cover (52 cases). The most probable reason for the contradictory estimate of the snow state is the difference between the areas (ROI) being considered for the visual inspections and the FSC estimations.

3.2. Comparison of FSC from Camera Imagery vs. SD from US

The comparison between the SD and FSC data in Sodankylä and Jokioinen indicated a rather good correlation between the two methods to produce snow presence information (Table 2). Approximately 17% of the data was contradictory (376 cases). This would mean around 10 mismatching cases per day with the used limits.

The study showed that there were clear differences between the behavior of the melting seasons of 2020 and 2021 in Sodankylä. Further visual inspection of the images showed that one reason was the melting of the snow under the SR50 sensor head during the melting season of 2020. The edge of the snow retreated towards the right side of the snowbed. The corresponding ROI (shown in Figure 2) was located a bit further from the SR50 spot, leading to the presence of snow based on the FSC information (FSC > 0% or FSC > 10%, see Table 4) in the cases where the SR50 indicated zero or very little snow.

Table 4. Comparison between FSC and SD data observed in Sodankylä and Jokioinen.

Observation Site	Snow Season	Number of Obs.	FSC = 0% SD ≥ 15 mm %/Cases	FSC ≤ 10% SD ≥ 15 mm %/Cases	FSC > 0% SD < 15 mm %/Cases	FSC > 10% SD < 15 mm %/Cases	Contradictory Cases/ Day (Based on Days/Season)
Sodankylä	melting 2020 (16 days)	147	0.7/1	0.7/1	29.9/44	23.1/34	3.0
Sodankylä	beginning 2020 (49 days)	192	1.0/2	2.1/4	2.6/5	2.6/5	0.2
Sodankylä	winter 2020–2021 (119 days)	827	0.0/6	0.1/17	0.0/0	0.0/0	0.1
Sodankylä	melting 2021 (48 days)	536	0.7/4	1.5/8	20.0/107	15.1/81	2.3
Jokioinen	beginning 2020 (20 days)	75	5.3/4	5.3/4	2.6/2	2.6/2	0.3
Jokioinen	winter 2020–2021 (47 days)	257	17.9/46	17.9/46	0.0/0	0.0/0	1.0
Jokioinen	melting 2021 (46 days)	241	1.2/3	1.2/3	56.0/135	37.3/93	3.0

In Jokioinen, during the winter season, the FSC showed a significant amount of “no snow” cases for the FSC data even though there was clearly snow for a long period based on the SD observations. Further visual inspection of the images proved that the most probable reason is darkness or diffuse shadows over the snow in images where image recognition is not able to predict the FSC correctly.

During the melting season in Jokioinen the high number of cases with no snow based on the SD data but indicative snow presence based on the FSC information was observed. The reason for this turned out to be reflections from the snow bed that were interpreted as snow by the image recognition algorithms.

3.3. Validity of FSC When SD from US Is Inaccurate

The correspondence between the visual inspection of snow presence and the FSC (based on the thresholds shown in Table 1) in Sodankylä and Jokioinen are presented in Tables 2 and 3, respectively. In addition, the comparison between the FSC and SD data are shown in Table 4. Here it must be noted that the handled data amount was quite small and included only one beginning, winter, and melting season in Jokioinen and one beginning and winter season and two melting seasons in Sodankylä. This increases the uncertainty of the analysis.

When the snow presence from the visual inspection is the reference, the FSC recognized the correct snow presence in Sodankylä efficiently: within melting seasons 2020 and 2021 approximately 94 percent of the results agreed with the visual inspection when the threshold

(TH) of the FSC was 0% (Table 5). When the TH of the FSC was increased to 10%, the detection accuracy decreased to ~77% and ~74% within the melting seasons of 2020 and 2021, respectively. This is mainly explained by the fact that reasonably the number of matching cases for the definition $FSC > 10\%$ and $2 \leq V \leq 3$ increased because the FSC values between 0 and 10% were neglected. In addition, the mismatching cases of the $FSC \leq 10\%$ and $2 \leq V \leq 3$ ensemble increased.

Table 5. Analysis results of the comparison between FSC data, SD data and visual inspection in Sodankylä and Jokioinen. TH% is the threshold of the FSC data to be taken into the analysis. V is the snow presence category from the visual inspection, values 1, 2 and 3 considered in the analysis.

Observation Site	Snow Season	Number of Obs.	FSC > TH%	FSC > TH%	FSC ≤ TH%	FSC ≤ TH%	Detection Accuracy When SD < 15 mm %
			SD < 15 mm V = 1 (False Positive) %/Cases TH = 0 TH = 10	SD < 15 mm V = 2 or 3 (True Positive) %/Cases TH = 0 TH = 10	SD < 15 mm V = 1 (True Negative) %/Cases TH = 0 TH = 10	SD < 15 mm V = 2 or 3 (False Negative) %/Cases TH = 0 TH = 10	
Sodankylä	melting 2020 (16 days)	147	1.4/2 0.7/1	28.6/42 22.4/33	1.4/2 2.0/3	0.7/1 6.8/10	93.6 76.6
Sodankylä	beginning 2020 (23 days)	75	0.0/0 0.0/0	0.0/0 0.0/0	0.0/0 0.0/0	0.0/0 0.0/0	N/A N/A
Sodankylä	winter 2020–2021 (119 days)	827	0.0/0 0.0/0	0.0/0 0.0/0	0.0/0 0.0/0	0.0/0 0.0/0	N/A N/A
Sodankylä	melting 2021 (48 days)	536	0.4/2 0.2/1	19.6/105 14.9/80	0.0/0 0.2/1	0.9/5 5.6/30	93.8 72.3
Sodankylä	All	1585	0.3/4 0.1/2	9.3/147 7.1/113	0.1/2 0.3/4	0.4/6 2.5/40	93.7 73.6
Jokioinen	beginning 2020 (20 days)	75	0.0/0 0.0/0	1.3/1 1.3/1	0.0/0 0.0/0	5.3/4 5.3/4	20.0 20.0
Jokioinen	winter 2020–2021 (47 days)	257	0.0/0 0.0/0	0.0/0 0.0/0	0.0/0 0.0/0	17.9/46 17.9/46	0.0 0.0
Jokioinen	melting 2021 (46 days)	241	15.6/37 9.3/22	40.9/97 29.5/70	4.1/10 10.4/25	1.2/3 1.2/3	72.8 79.2
Jokioinen	All	573	6.5/37 3.8/22	17.1/98 12.4/71	1.7/10 4.2/24	9.2/53 9.2/53	54.5 55.9
All	melting combined	924	4.4/41 2.6/24	26.4/244 19.8/183	1.3/12 3.1/29	1.0/9 4.7/43	83.7 76.0
All	All	2158	1.9/41 1.1/24	11.4/245 8.5/184	0.6/12 1.3/28	2.7/59 4.3/93	72.0 64.4

Within the beginning and winter seasons there were no cases where all the set definitions were met, presumably because of the low number of SD < 15 mm cases and the fact that FSC and SD correspond well when SD >> 0 mm.

The detection accuracy of the FSC information in Jokioinen deviated between the seasons for the cases where SD < 15 mm (Table 5). The beginning of season 2020 included a small number of cases in all the ensembles of the FSC and V with a remarkable part in the situation where the FSC informs no snow and the visual inspection estimates full or partly snow cover. Thus, the detection accuracy was only 20%. Within the winter season 2020–2021 a significant number of cases were recognized when the $FSC \leq TH\%$ and $2 \leq V \leq 3$ (46 cases of all the 257 observations, 18%). The same behavior was observed when the FSC was compared with the SD > 15 mm (Table 4). This was presumably due to the unclear images that were not recognized by the FSC algorithm.

For the melting season of 2021, the detection accuracy of the FSC was rather good, ~73% and 79% for the TH = 0% and TH = 10%, respectively. Here, when the FSC recognized some snow and the visual inspection did not, the number of cases was significant. This contradictory behavior was also seen between the SD and the FSC. It was determined by manually checking several images that the reason for the mismatching estimations was the reflection from the snowbed that was incorrectly recognized to be snow.

A combined performance of the two stations results in 72% and ~64% for the TH = 0% and TH = 10%, respectively, for all the seasons combined and ~84% and ~76% for the TH = 0% and TH = 10%, respectively, for melting the seasons combined. Although the higher threshold (10%) works better for Jokioinen, the overall accuracy of ~84% for the melting season is considerably high for the two stations combined with 0% TH.

4. Discussion

The FSC information presented in Chapter 2.5 was successfully produced using the FMIPROT toolbox. The FOVs with the chosen ROIs are shown in Figure 1. As described in Chapter 2.10, the FSC data are transmitted to the test collection of the operational database of the FMI. The FSC data are freely available via the FMIPROT interface and for the FMI personnel via test tables (i.e., as an experimental dataset) of the database every 10 min.

The pilot project gave promising results to the possibilities of the FSC data. Even though there clearly are some challenges in image recognition in certain cases the data are mostly good quality and corresponds well with the SD observations as well as the visual inspection for snow presence from the images. The project gave a good overview of the cases where the image recognition algorithms could still be developed e.g., to detect and filter out the images where it is hard to predict the snow presence more efficiently.

The comparison between the SD and FSC data showed clear evidence of the benefits of using FSC information to complement the SD data in the cases where the SD information is known to be uncertain. It is shown that when the US derived SD is less than 2 cm in the melting season, the webcam derived FSC can be used to recognize snow presence. On the other hand, the performance has a difference between the two stations and between different the FSC thresholds. Those differences may be caused by the visual inspection coverage differing from the ROI of the FSC estimation or even the color composition of the camera views or the camera quality, which would affect the brightness distribution of the ROI. In addition, the project recognized the cases that need further investigations. The study should be repeated in more stations with different cameras, land cover, and terrain, as well as considering different ROI selections (e.g., outside snowbed) to evaluate in what kind of environment the method can be applied. Additionally, using different FSC detection methods, such as classification by machine learning, can be considered to pursue a better performance. The developed system that processes and feeds the interpreted FSC data to the test collection of the operational database enables the easier handling of the data for the established users and makes the utilization of the new FSC data in operations.

Based on the positive findings and the observed quality of the FSC information, the authors recommend taking further steps to apply the FSC information into the operational data production system. Further, the positive outcomes should be utilized in the discussions with the various users to promote the usage of FSC information and to identify the users' needs more closely, e.g., specific derived on/off variables.

Author Contributions: Conceptualization, A.F., A.N.A., C.M.T., E.L., K.L. and L.L.; methodology, A.F., A.N.A., C.M.T., E.L., K.L. and L.L.; software, C.M.T.; validation, A.F. and E.L.; formal analysis, A.F. and E.L.; investigation, A.F., C.M.T. and E.L.; resources, A.F., C.M.T., K.L. and L.L.; data curation, A.F. and C.M.T.; writing—original draft preparation, C.M.T.; writing—review and editing, A.F., A.N.A., C.M.T., E.L., K.L. and L.L.; visualization, A.F., C.M.T. and E.L.; supervision, A.N.A., K.L. and L.L.; project administration, K.L. and L.L. All authors have read and agreed to the published version of the manuscript.

Funding: This research received no external funding.

Data Availability Statement: Camera images used in this study are unavailable due to data policy and data management restrictions. Processing software and processing options (setup content and files) are available in fmiprot.fmi.fi, as a guide to apply the studied method to similar camera imagery. Processing options in fmiprot.fmi.fi are subject to change without notice. Processing results of the setups are also available in fmiprot.fmi.fi, but the temporal range of data changes due to NRT processing and the data may change due to changes in setup options.

Acknowledgments: The authors acknowledge Saila Mastosalo and Mirja Kirjavainen for their meticulous work in visual inspection of the images and Jokioinen station staff for the installation of the camera and establishing the data flow.

Conflicts of Interest: The authors declare no conflict of interest. The funders had no role in the design of the study; in the collection, analyses, or interpretation of data; in the writing of the manuscript; or in the decision to publish the results.

References

1. Pirazzini, R.; Leppänen, L.; Picard, G.; Lopez-Moreno, J.I.; Marty, C.; Macelloni, G.; Kontu, A.; von Lerber, A.; Tanis, C.M.; Schneebeli, M.; et al. European In-Situ Snow Measurements: Practices and Purposes. *Sensors* **2018**, *18*, 2016. [[CrossRef](#)] [[PubMed](#)]
2. Bongio, M.; Arslan, A.N.; Tanis, C.M.; De Michele, C. Snow depth time series retrieval by time-lapse photography: Finnish and Italian case studies. *Cryosphere* **2021**, *15*, 369–387. [[CrossRef](#)]
3. Salvatori, R.; Plini, P.; Giusto, M.; Valt, M.; Salzano, R.; Montagnoli, M.; Cagnati, A.; Crepaz, G.; Sigismondi, D. Snow cover monitoring with images from digital camera systems. *Ital. J. Remote Sens.* **2011**, *43*, 137–145. [[CrossRef](#)]
4. Arslan, A.N.; Tanis, C.M.; Metsämäki, S.; Aurela, M.; Böttcher, K.; Linkosalmi, M.; Peltoniemi, M. Automated Webcam Monitoring of Fractional Snow Cover in Northern Boreal Conditions. *Geosciences* **2017**, *7*, 55. [[CrossRef](#)]
5. Tanis, C.M.; Peltoniemi, M.; Linkosalmi, M.; Aurela, M.; Böttcher, K.; Manninen, T.; Arslan, A.N. A System for Acquisition, Processing and Visualization of Image Time Series from Multiple Camera Networks. *Data* **2018**, *3*, 23. [[CrossRef](#)]
6. Jokinen, P.; Pirinen, P.; Kaukoranta, J.P.; Kangas, A.; Alenius, P.; Eriksson, P.; Johansson, M.; Wilkman, S. *Tilastoja Suomen Ilmastosta ja Merestä 1991–2020*; Finnish Meteorological Institute: Helsinki, Finland, 2021; Volume 8. [[CrossRef](#)]
7. Nitu, R.; Roulet, Y.A.; Wolff, M.; Earle, M.E.; Reverdin, A.; Smith, C.D.; Kochendorfer, J.; Morin, S.; Rasmussen, R.; Wong, K.; et al. *WMO Solid Precipitation Intercomparison Experiment (SPICE) (2012–2015)*; World Meteorological Organization: Geneva, Switzerland, 2019. Available online: <http://hdl.handle.net/20.500.11765/10839> (accessed on 13 February 2023).
8. *Guide to Instruments and Methods of Observation, Volume I—Measurement of Meteorological Variables, 2018 Edition*; World Meteorological Organization: Geneva, Switzerland, 2018; pp. 21–26.
9. Lakkala, K.; Jaros, A.; Aurela, M.; Tuovinen, J.-P.; Kivi, R.; Suokanerva, H.; Karhu, J.M.; Laurila, T. Radiation measurements at the Pallas-Sodankylä Global Atmosphere Watch station—Diurnal and seasonal cycles of ultraviolet, global and photosynthetically-active radiation. *Boreal Environ. Res.* **2016**, *21*, 427–444. Available online: <http://hdl.handle.net/10138/225785> (accessed on 13 February 2023).
10. *SR50A/AT Sonic Ranging Sensor: User Manual*; Campbell Scientific Ltd.: Loughborough, UK, 2011; p. 2.

Disclaimer/Publisher’s Note: The statements, opinions and data contained in all publications are solely those of the individual author(s) and contributor(s) and not of MDPI and/or the editor(s). MDPI and/or the editor(s) disclaim responsibility for any injury to people or property resulting from any ideas, methods, instructions or products referred to in the content.